

# Surface bound states in $n$ -band systems with the quasiclassical approach

Yuki Nagai

*Department of Physics, University of Tokyo, Tokyo 113-0033, Japan  
and TRIP, JST, Chiyoda, Tokyo 102-0075, Japan*

Nobuhiko Hayashi

*Nanoscience and Nanotechnology Research Center (N2RC), Osaka Prefecture University,  
1-2 Gakuen-cho, Naka-ku, Sakai 599-8570 Osaka, Japan  
and CREST (JST), 4-1-8 Honcho, Kawaguchi, Saitama 332-0012, Japan*

(Received 17 March 2009; published 9 June 2009)

We discuss the tunneling spectroscopy at a surface in multiband systems such as Fe-based superconductors with the use of the quasiclassical approach. We extend the single-band method by M. Matsumoto and H. Shiba [J. Phys. Soc. Jpn. **64**, 1703 (1995)] into  $n$ -band systems ( $n \geq 2$ ). We show that the appearance condition of the zero-bias conductance peak does not depend on details of the pair-potential anisotropy, but it depends on details of the normal-state properties in the case of fully gapped superconductors. The surface density of states in a two-band superconductor is presented as a simplest application. The quasiclassical approach enables us to calculate readily the surface-angular dependence of the tunneling spectroscopy.

DOI: [10.1103/PhysRevB.79.224508](https://doi.org/10.1103/PhysRevB.79.224508)

PACS number(s): 74.20.Rp, 74.25.Op, 74.25.Bt

## I. INTRODUCTION

Much attention has been focused on novel Fe-based superconductors since the recent discovery of superconductivity at the high temperature of 26 K in  $\text{LaFeAsO}_{1-x}\text{F}_x$ .<sup>1</sup> Many theoretical and experimental studies on Fe-based superconductors have been reported in the last year. It is important to identify the superconducting order parameter to elucidate the mechanism of superconductivity in those high- $T_c$  materials.

A  $\pm s$ -wave pairing symmetry has been theoretically proposed as one of the candidates for the pairing symmetry in Fe-pnictide superconductors.<sup>2-11</sup> The  $\pm s$ -wave symmetry means that the symmetry of pair potentials on each Fermi surface is  $s$  wave and the relative phase between them is  $\pi$ . Recently, we showed that a fully gapped anisotropic  $\pm s$ -wave superconductivity consistently explained experimental observations such as nuclear magnetic relaxation rate and superfluid density.<sup>12</sup>

A key point to identify the  $\pm s$ -wave symmetry is a detection of the sign change in the order parameters between Fermi surfaces. It is difficult to detect the relative phase of the order parameters in a bulk material. However, as shown in studies of high- $T_c$  cuprates, Andreev bound states are formed at a surface or a junction when the quasiparticles feel different signs of the order parameter before and after scattering.<sup>13-15</sup> Since one can extract the information on the relative phase through Andreev bound states, several theoretical studies on junctions and surfaces have been reported recently.<sup>16-24</sup> Andreev bound states at zero energy have been experimentally observed as a zero-bias conductance peak (ZBCP) in tunneling spectroscopy for Fe-based superconductors.<sup>25</sup>

The Fe-based superconductors are also interesting as novel unconventional multiband superconductors since multiband effects are essentially important there.<sup>3</sup> Fermi surfaces in these systems predominantly consist of the  $d$  orbitals of Fe atom. Kuroki *et al.*<sup>3</sup> suggest that five orbitals are necessary to describe the properties of the superconductivity and

they elaborate an effective five-band model. On the other hand,  $\text{MgB}_2$  is a two-band system that is a conventional  $s$ -wave BCS-type superconductor.

The aim of this paper is to develop a method for analyzing surface bound states in multiband superconductors. Matsumoto and Shiba<sup>26</sup> developed a method to analyze surface bound states in single-band systems such as high- $T_c$  cuprates. We extend their method into multiband systems. Since the ratio of the superconducting gap  $\Delta$  to the Fermi energy  $E_F$  is small  $\Delta/E_F \ll 1$  in Fe-based superconductors, we can adopt a quasiclassical approach. In this approach, all we need is only to consider quasiparticles at the Fermi level. Thus, we can reduce computational machine time and the physical picture becomes clear. In addition, this approach enables us to easily calculate the surface-angular dependence of tunneling spectroscopy. We find a general appearance condition of the ZBCP for multiband systems. This general condition can be applied to various pairing symmetries including  $\pm s$  wave and  $d$  wave. With our method, we will discuss a two-band superconductor as a simple example.

This paper is organized as follows. The formulation of our quasiclassical approach is shown in Sec. II. We apply a quasiclassical approximation to eliminate fast spatial oscillations with Fermi wavelength. The appearance condition of the ZBCP in multiband systems is derived in Sec. III. The results for a two-band model are shown as a simple example of our approach in Sec. IV, where we will show both analytical and numerical results. The discussions and conclusion are given in Secs. V and VI, respectively. In the Appendix, we describe the derivation of the appearance condition of the ZBCP when a system can be treated without quasiclassical approximation.

## II. FORMULATION

### A. Orbital representation and band representation

Let us consider the local density of states near a surface following a procedure by Matsumoto and Shiba.<sup>26</sup> We as-

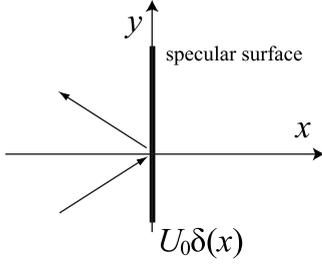


FIG. 1. Figure of a specular surface.

sume a two-dimensional superconductor and consider a specular surface for which the component of the quasiparticle momentum along the surface is conserved as shown in Fig. 1. We treat the surface as a potential  $U(\mathbf{r})\check{\tau}_3$  where the time-reversal symmetry is conserved.<sup>26</sup> Here,  $\check{\tau}_i (i=1,2,3)$  denote Pauli matrices in Nambu space and  $\mathbf{r}$  is the position in the real space. We consider a  $n$ -orbital system which is a periodic crystal with  $n$  atomic orbitals in unit cell. Throughout the paper,  $\hat{a}$  denotes a  $n \times n$  matrix in the orbital space and  $\check{a}$  denotes a  $2n \times 2n$  matrix composed of the  $2 \times 2$  Nambu space and the  $n \times n$  orbital space. We calculate the Green's function under the influence of  $U(\mathbf{r})\check{\tau}_3$ . It is written as

$$\check{G}(\mathbf{r}, \mathbf{r}') = \check{G}_0(\mathbf{r}, \mathbf{r}') + \int d\mathbf{r}'' \check{G}_0(\mathbf{r}, \mathbf{r}'') U(\mathbf{r}'') \check{\tau}_3 \check{G}(\mathbf{r}'', \mathbf{r}). \quad (1)$$

Here  $\check{G}_0$  is an unperturbed Green's function in the absence of  $U$ . We take the  $x(y)$ -axis perpendicular (parallel) to the surface as shown in Fig. 1. Considering the surface situated at  $x=0$  and the scattering potential  $U$  written as  $U(\mathbf{r})=U_0\delta(x)$ , Eq. (1) is reduced to

$$\check{G}(x, k_y, x', k'_y) = 2\pi\delta(k_y - k'_y)\check{G}(x, x', k_y), \quad (2)$$

where

$$\begin{aligned} \check{G}(x, x', k_y) &= \check{G}_0(x, x', k_y) + \check{G}_0(x, 0, k_y) U_0 \check{\tau}_3 \\ &\times [1 - \check{G}_0(0, 0, k_y) U_0 \check{\tau}_3]^{-1} \check{G}_0(0, x', k_y). \end{aligned} \quad (3)$$

Here we have taken the Fourier transformation with respect to  $y$ . We use units in which  $\hbar=1$  and the coordinates  $\mathbf{r}$  and the momentum  $\mathbf{k}$  are dimensionless. The surface is actually represented in the limit  $U_0 \rightarrow \infty$ . The Green's function is then given by

$$\check{G}(x, x', k_y) = \check{G}_0(x, x', k_y) + \check{G}_P(x, x', k_y), \quad (4)$$

where

$$\check{G}_P(x, x', k_y) \equiv -\check{G}_0(x, 0, k_y) \check{G}_0(0, 0, k_y)^{-1} \check{G}_0(0, x', k_y). \quad (5)$$

The local density of states at the position  $x$  for the momentum  $k_y$  is written as

$$N(x, k_y) = -\frac{1}{\pi} \text{Im}[\text{Tr} \hat{G}^R(x, x, k_y)], \quad (6)$$

where

$$\hat{G}^R(x, x, k_y) = \hat{G}(x, x, k_y)|_{i\omega_m \rightarrow E+i\eta}. \quad (7)$$

Here  $\omega_m$  is the fermion Matsubara frequency and  $\eta$  is a positive infinitesimal quantity. The unperturbed Green's function  $\check{G}_0^R(x, x', k_y)$  is given by

$$\check{G}_0^R(x, x', k_y) = \frac{1}{2\pi} \int dk_x e^{ik_x(x-x')} \check{G}_0^R(k_x, k_y), \quad (8)$$

where

$$\check{G}_0^R(k_x, k_y) = [E - \check{H}_N^o(k_x, k_y)]^{-1}. \quad (9)$$

Here,  $\check{H}_N^o(k_x, k_y)$  is the  $2n \times 2n$  Hamiltonian in Nambu and orbital spaces written as

$$\check{H}_N^o \equiv \begin{pmatrix} \hat{H}^o & \hat{\Delta}^o \\ \hat{\Delta}^{o\dagger} & -\hat{H}^o \end{pmatrix} \quad (10)$$

in the ‘‘orbital representation’’ where the base functions are atomic orbitals in crystal unit cell. From now on, the subscript ‘‘o’’ indicates that matrices are represented with the orbital basis.  $\hat{H}^o$  is the Hamiltonian in the normal state represented as  $n \times n$  matrix in the orbital space. Remember that  $n$  is the number of the orbitals.  $\hat{\Delta}^o$  is the superconducting order parameter.

Let us introduce a  $n \times n$  Hamiltonian in the ‘‘band representation’’ defined by

$$\hat{H}^b(k_x, k_y) \equiv \hat{P}^{-1}(k_x, k_y) \hat{H}^o(k_x, k_y) \hat{P}(k_x, k_y) \quad (11)$$

$$= \begin{pmatrix} \lambda_1 & 0 & 0 \\ 0 & \ddots & 0 \\ 0 & 0 & \lambda_n \end{pmatrix}. \quad (12)$$

Here  $\lambda_i (i=1, 2, \dots, n)$  denote the eigenvalues where the relation  $\lambda_i > \lambda_j (i < j)$  is satisfied.  $\hat{P}$  is a unitary matrix that consists of the eigenvectors that diagonalizes the Hamiltonian  $\hat{H}^o$ . The  $2n \times 2n$  Hamiltonian in Nambu and orbital spaces in the band representation is also defined by

$$\check{H}_N^b(k_x, k_y) \equiv \check{U}^{-1}(k_x, k_y) \check{H}_N^o(k_x, k_y) \check{U}(k_x, k_y) \quad (13)$$

$$= \begin{pmatrix} \hat{H}^b & \hat{\Delta}^b \\ \hat{\Delta}^{b\dagger} & -\hat{H}^b \end{pmatrix}, \quad (14)$$

where

$$\check{U}(k_x, k_y) \equiv \begin{pmatrix} \hat{P}(k_x, k_y) & 0 \\ 0 & \hat{P}(k_x, k_y) \end{pmatrix}, \quad (15)$$

$$\hat{\Delta}^b \equiv \hat{P}^{-1} \hat{\Delta}^o \hat{P}. \quad (16)$$

In general,  $\hat{\Delta}^b$  contains off-diagonal elements which correspond to interband pairings. Assuming that intraband pairings are dominant, we neglect the off-diagonal (interband) elements in  $\hat{\Delta}^b$

$$\hat{\Delta}^b \approx \begin{pmatrix} \Delta_1 & 0 & 0 \\ 0 & \ddots & 0 \\ 0 & 0 & \Delta_n \end{pmatrix}. \quad (17)$$

That is, we consider that only single pair potential is defined on each Fermi surface. Here,  $\Delta_i$  is the pair potential on the  $i$ th band. Substituting Eq. (13) into Eq. (9), the Green's function  $\check{G}_0^R(k_x, k_y)$  is written as

$$\check{G}_0^R(k_x, k_y) = \check{U}(E - \check{H}^b)^{-1} \check{U}^{-1}. \quad (18)$$

Assuming Eq. (17) and taking the inverse matrix of  $E - \check{H}^b$ , one can obtain

$$\check{G}_0^R(k_x, k_y) = \check{U} \begin{pmatrix} \hat{A}_+ & \hat{B} \\ \hat{B}^\dagger & \hat{A}_- \end{pmatrix} \check{U}^{-1}, \quad (19)$$

where

$$\hat{A}_\pm = \begin{pmatrix} \frac{E \pm \lambda_1}{-|\Delta_1|^2 + E^2 - \lambda_1^2} & 0 & 0 \\ 0 & \ddots & 0 \\ 0 & 0 & \frac{E \pm \lambda_n}{-|\Delta_n|^2 + E^2 - \lambda_n^2} \end{pmatrix}, \quad (20)$$

$$\hat{B} = \begin{pmatrix} \frac{\Delta_1}{-|\Delta_1|^2 + E^2 - \lambda_1^2} & 0 & 0 \\ 0 & \ddots & 0 \\ 0 & 0 & \frac{\Delta_n}{-|\Delta_n|^2 + E^2 - \lambda_n^2} \end{pmatrix}. \quad (21)$$

We find that Eq. (19) can be rewritten as

$$\check{G}_0^R(k_x, k_y) = \sum_i \check{G}^i(k_x, k_y), \quad (22)$$

where  $i$  is the band index and

$$\check{G}^i \equiv \frac{1}{-|\Delta_i|^2 + E^2 - \lambda_i^2} \begin{pmatrix} (E + \lambda_i) \hat{M}_i & \Delta_i \hat{M}_i \\ \Delta_i^* \hat{M}_i & (E - \lambda_i) \hat{M}_i \end{pmatrix}, \quad (23)$$

$$[\hat{M}_i]_{jk} = [\hat{P}]_{ji} [\hat{P}]_{ki}^*. \quad (24)$$

Equation (22) is divided into a sum of the Green's functions defined on each band. Substituting Eq. (22) into Eq. (8),  $\check{G}_0^R(x, x', k_y)$  is expressed as

$$\check{G}_0^R(x, x', k_y) = \sum_i \frac{1}{2\pi} \int dk_x e^{ik_x(x-x')} \check{G}^i(k_x, k_y). \quad (25)$$

Hence the  $k_x$  integration is found to be performed on each band independently.

### B. Quasiclassical approach

We assume  $|\Delta_i| \ll E_F$ . This relation is satisfied in most of systems such as conventional superconductors and Fe-based

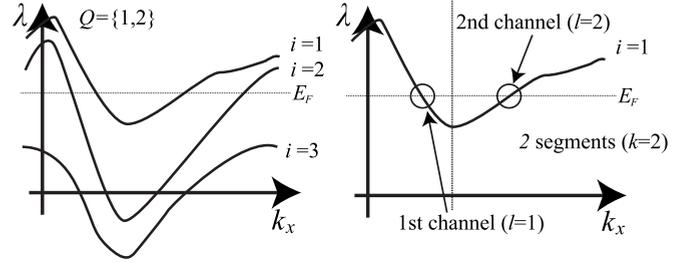


FIG. 2. Figures of band dispersions along a  $k_x$  line with a fixed  $k_y$ .

ones. In this case, one can use a quasiclassical approach.

We consider a line with a fixed  $k_y$  in the momentum space. On this line, we classify  $n$  bands into two groups. One group is composed of the bands on which the eigen energy  $\lambda_i(k_x, k_y)$  crosses the Fermi level (for example, the bands  $i=1$  and 2 in Fig. 2). The other group is composed of the bands on which the eigenenergy does not cross the Fermi level (the band  $i=3$ ). For the former group, we can analytically integrate  $\check{G}^i(k_x, k_y)$  over  $k_x$  with the use of a quasiclassical approach since  $\check{G}^i(k_x, k_y)$  is a function localized near the Fermi level. For the latter group, we need to integrate  $\check{G}^i(k_x, k_y)$  over  $k_x$  numerically since  $\check{G}^i(k_x, k_y)$  is not a localized function. However, the integrand is a smooth function so that it is easy to perform such a numerical integration.

We integrate  $\check{G}^i(k_x, k_y)$  on the bands of the first group with the use of the quasiclassical approach. To perform the  $k_x$  integration, we divide the  $k_x$  line with a fixed  $k_y$  into some segments as shown in Fig. 2. Each segment has only single channel that is the point satisfying the relation  $\lambda_i = E_F$ . From now on,  $l$  denotes the channel index and  $k$  denotes the maximum number of  $l$ . The integration for the  $i$ th band is written as

$$\int dk_x \sim \sum_{l=1}^k \int_{-\infty}^{\infty} \frac{d\lambda_i}{v_i(\lambda_i)}. \quad (26)$$

Expanding  $k_x(\lambda_i)$  in the first order of  $\lambda_i$  around  $\lambda_i = E_F$  as  $k_x(\lambda_i) = k_{Fx} + \lambda_i / v_{Fx}$ , one can carry out the integration by the residue theorem

$$\frac{1}{2\pi} \int dk_x e^{ik_x(x-x')} \check{G}^i(k_x, k_y) = -i \sum_{l=1}^k \check{G}_{i,l}^F(k_{Fx}^{i,l}), \quad (27)$$

where

$$\check{G}_{i,l}^F(k_{Fx}^{i,l}) \equiv \frac{e^{ik_{Fx}^{i,l}(x-x')} e^{i|x-x'| \sqrt{E^2 - |\Delta_i|^2} / |v_{Fx}^{i,l}|}}{2|v_{Fx}^{i,l}| \sqrt{E^2 - |\Delta_i|^2}} \check{F}(k_{Fx}^{i,l}), \quad (28)$$

$$\check{F}(k_{Fx}^{i,l}) \equiv \begin{pmatrix} f_+(k_{Fx}^{i,l}) \hat{M}_i(k_{Fx}^{i,l}) & \Delta_i(k_{Fx}^{i,l}) \hat{M}_i(k_{Fx}^{i,l}) \\ \Delta_i(k_{Fx}^{i,l}) \hat{M}_i(k_{Fx}^{i,l}) & f_-(k_{Fx}^{i,l}) \hat{M}_i(k_{Fx}^{i,l}) \end{pmatrix}, \quad (29)$$

$$f_{\pm}(k_{Fx}^{i,l}) \equiv E \pm \text{sgn}(x-x') \text{sgn}(v_{Fx}^{i,l}) \sqrt{E^2 - |\Delta_i|^2}. \quad (30)$$

Here,  $k_{Fx}^{i,l}$  and  $v_{Fx}^{i,l}$  are the Fermi wave number and the Fermi velocity on the  $l$ th channel, respectively. Using the above, Eq. (25) can be written as

$$\begin{aligned} \check{G}_0^R(x, x', k_y) = & -i \sum_{i \in Q} \sum_{l=1}^k \check{G}_{i,l}^F(x, x', k_{Fx}^{i,l}) \\ & + \sum_{i \notin Q} \frac{1}{2\pi} \int dk_x e^{ik_x(x-x')} \check{G}^i(k_x, k_y), \end{aligned} \quad (31)$$

where the elements in  $Q$  are the indices of the bands whose energy dispersions cross the Fermi level for a fixed  $k_y$ . Here we assume  $\Delta_{i \in Q} = 0$ , namely, the superconducting order parameters are finite only around the Fermi level. It should be noted that the second term on the right-hand side of Eq. (31) cannot be neglected since  $\check{G}_0^R(0, 0, k_y)^{-1}$  without this second term may have artificial divergences.

### C. Eliminating the fast oscillations with Fermi wavelength

We assume the condition  $k_F \xi \gg 1$  (i.e.,  $|\Delta_i| \ll E_F$ ) which is the quasiclassical condition. Here  $\xi$  is the coherence length of a superconductor. Under this condition, the short-range spatial oscillations characterized by the Fermi wavelength  $1/k_F$  can be eliminated. We rewrite Eq. (31) as

$$\check{G}_0^R(x, x', k_y) = \sum_i \int dk_x \check{K}_i(k_x, k_y) e^{ik_x(x-x')}, \quad (32)$$

where

$$\check{K}_{i \in Q}(k_x, k_y) \equiv -i \sum_l^k G_{i,l}^F(x, x', k_x) \delta(k_x - k_{Fx}^{i,l}), \quad (33)$$

$$\check{K}_{i \notin Q}(k_x, k_y) \equiv \frac{1}{2\pi} \check{G}^i(k_x, k_y). \quad (34)$$

The perturbed Green's function  $\check{G}_P(x, x', k_y)$  defined in Eq. (5) can be written as

$$\begin{aligned} \check{G}_P^R(x, x', k_y) = & - \sum_{i,i''} \int dk_x dk_x'' e^{i(k_x x - k_x'' x')} \check{K}_i(k_x, k_y) \\ & \times \check{G}_0^R(0, 0, k_y)^{-1} \check{K}_{i''}(k_x'', k_y). \end{aligned} \quad (35)$$

Setting  $\exp[i(k_x x - k_x'' x')] \rightarrow 1$ , we eliminate the short-range oscillation while keeping the enveloping profile of the integrand. Thus, the above equation is reduced to

$$\begin{aligned} \check{G}_P^R(x, x', k_y) = & - \sum_i \int dk_x \check{K}_i(k_x, k_y) \check{G}_0^R(0, 0, k_y)^{-1} \\ & \times \sum_{i''} \int dk_x'' \check{K}_{i''}(k_x'', k_y). \end{aligned} \quad (36)$$

From this equation, it is concluded that the Andreev bound states appear when  $\check{G}_0^R(0, 0, k_y)^{-1}$  diverges, i.e., when  $\det \check{G}_0^R(0, 0, k_y) = 0$ .

### III. APPEARANCE CONDITION OF THE ZBCP

Let us consider the appearance condition of the ZBCP in  $n$ -band system at a surface. At the zero energy  $E=0$ ,  $\check{G}_{i,l}^F(x=0, x'=0, k_{Fx}^{i,l})$  defined in Eq. (28) (for  $i \in Q$ ) is written as

$$\check{G}_{i,l}^F(k_{Fx}^{i,l}) = \frac{\text{sgn}(\Delta_i)}{2|v_{Fx}^{i,l}|} \begin{pmatrix} 0 & \hat{M}_i(k_{Fx}^{i,l}) \\ \hat{M}_i(k_{Fx}^{i,l}) & 0 \end{pmatrix}. \quad (37)$$

For  $i \notin Q$ , we have from Eq. (23) with  $E=0$ ,

$$\check{G}^i = \frac{1}{-\lambda_i^2} \begin{pmatrix} \lambda_i \hat{M}_i & 0 \\ 0 & -\lambda_i \hat{M}_i \end{pmatrix}, \quad (38)$$

where we have set  $\Delta_i=0$  because the superconducting order parameter is assumed to be finite only near the Fermi level and the bands with the indices  $i \notin Q$  do not cross it. Substituting the above equations into Eq. (31), we can obtain the appearance condition of the ZBCP from  $\det \check{G}_0^R(0, 0, k_y) = 0$  as

$$\det \begin{pmatrix} -\hat{I} & \hat{L} \\ \hat{L} & \hat{I} \end{pmatrix} = 0, \quad (39)$$

where

$$\hat{L} \equiv -i \sum_{i \in Q} \sum_l \frac{\text{sgn}[\Delta_i(k_{Fx}^{i,l})]}{2|v_{Fx}^{i,l}|} \hat{M}_i(k_{Fx}^{i,l}), \quad (40)$$

$$\hat{I} \equiv \sum_{i \notin Q} \frac{1}{2\pi} \int \frac{dk_x}{\lambda_i(k_x)} \hat{M}_i(k_x). \quad (41)$$

Equation (40) shows that the appearance condition *does not* depend on the anisotropy of the pair potentials and it depends only on their signs because information on the pair potentials is included in the form  $\text{sgn}[\Delta_i(k_{Fx}^{i,l})]$  in Eq. (40). This result shows that information on the normal state (i.e., the matrices  $\hat{M}_i$  and  $v_{Fx}^{i,l}$ ) is important for the ZBCP to appear.

### IV. TWO-BAND MODEL AS A SIMPLE EXAMPLE

#### A. Model

We calculate the density of states in a two-band superconductor as a simple example. We consider a two-band tight-binding model on a square lattice. There are two orbitals on each lattice site. The Hamiltonian with a  $2 \times 2$  matrix form in the normal state is described as

$$\hat{H}^o = \begin{pmatrix} -t \cos(k_a) - \mu & 2t' \sin(k_a) \sin(k_b) \\ 2t' \sin(k_a) \sin(k_b) & -t \cos(k_b) - \mu \end{pmatrix}, \quad (42)$$

in the orbital representation ( $n=2$ ). Here  $k_a$  and  $k_b$  are the axes fixed to the crystal axes in the momentum space,  $t$  and  $t'$  are intraorbital and interorbital hopping amplitudes, respectively, and  $\mu$  denotes the chemical potential. We use the unit in which the lattice constant  $a=1$ . This Hamiltonian can be diagonalized into the matrix in the band representation  $\hat{H}^b$ , written as

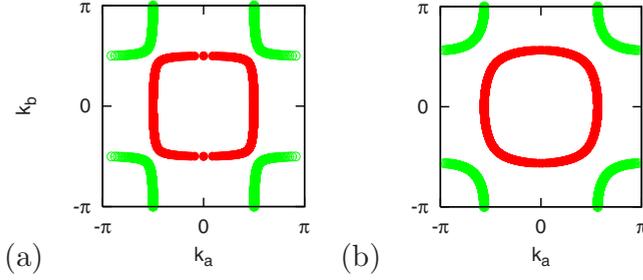


FIG. 3. (Color online) Fermi surfaces in the two-band model. (a) The half filling ( $\mu=0$ ) and  $t'=0.1t$ . (b)  $\mu=0.2t$  and  $t'=0.2t$ .

$$\hat{H}^b = \hat{P}^{-1} \hat{H}^o \hat{P} = \begin{pmatrix} \lambda_A & 0 \\ 0 & \lambda_B \end{pmatrix}. \quad (43)$$

Here  $\lambda_{A(B)}$  denotes the energy dispersion on the  $A(B)$  band. As shown in Fig. 3, the Fermi surfaces consist of two parts near the half filling.

We consider the two-band  $s$ -wave superconductor described by the pair potential in the band representation

$$\hat{\Delta}^b = \begin{pmatrix} \Delta_A & 0 \\ 0 & \Delta_B \end{pmatrix}. \quad (44)$$

Here  $\Delta_{A(B)}$  is the pair potential on the  $A(B)$  band.

We introduce the coordinates  $(k_a, k_b)$  fixed to the crystal axes

$$\begin{pmatrix} k_a \\ k_b \end{pmatrix} = \begin{pmatrix} \cos \theta & -\sin \theta \\ \sin \theta & \cos \theta \end{pmatrix} \begin{pmatrix} k_x \\ k_y \end{pmatrix}. \quad (45)$$

Here the  $k_x(k_y)$  axis is the axis parallel (perpendicular) to the surface and  $\theta$  is the angle between the  $k_a$  and  $k_x$  axes. Considering  $[110]$  surface, we fix  $\theta=\pi/4$ . The quasiparticle momentum  $k_y$  is conserved since we consider the specular surface.

It should be noted that one needs to treat the Brillouin zone in the surface coordinates  $(k_x, k_y)$  for each surface angle since it is necessary to consider all possible scattering processes at the specular surface (namely, all  $k_y$ -momentum-conserving processes). For example, it naively seems in Fig. 3(a) that possible scattering processes occur only on the inner Fermi surface (red) for the  $[110]$  surface ( $\theta=\pi/4$ ) in the region  $\pi\sqrt{2}/4 < k_y < \pi\sqrt{2}/2$  [the  $k_y$  axis is directed in the direction of  $(k_a, k_b)=(-1, 1)$  in Fig. 3(a)]. However for  $[110]$  surface, one has to also consider the outside of the first Brillouin zone as shown in Fig. 4 so that the scattering process between the outer Fermi surface (green) and the inner Fermi surface (red) can occur.

At the half filling for  $[110]$  surface, the second term in Eq. (31) does not exist since the energy dispersions of the  $A$  and  $B$  bands always cross the Fermi level on  $k_x$  line with any fixed  $k_y$  in the momentum space as shown in Fig. 4. In this case,  $\hat{L}$  defined in Eq. (41) is zero because there is no band with the index  $i \notin Q$ . Therefore, the appearance condition of the ZBCP in Eq. (39) can be rewritten as

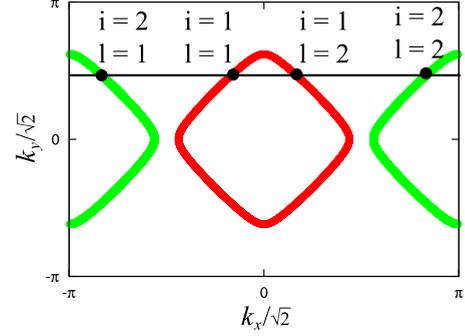


FIG. 4. (Color online) Fermi surfaces ( $\mu=0$  and  $t'=0.1t$ ) and  $k_x$  line with fixed  $k_y$ .

$$\det \hat{L} = 0, \quad (46)$$

where  $\hat{L}$  is defined in Eq. (40).

## B. Analytical results

### 1. At the half filling for $[110]$ surface

We will analytically show that the ZBCP always appears for any strength of the interorbital hopping  $t'$  in the case of  $[110]$  surface ( $\theta=\pi/4$ ) at the half filling. On the lines which satisfy  $k_a=(k_x-k_y)/\sqrt{2}=n\pi$  or  $k_b=(k_x+k_y)/\sqrt{2}=n\pi$  in the momentum space, one can easily obtain the unitary matrix  $\hat{P}$  that diagonalizes  $\hat{H}^o$

$$\hat{P}(k_y) = \begin{cases} \begin{pmatrix} 1 & 0 \\ 0 & 1 \end{pmatrix}, & k_x - k_y = n_e \pi \text{ or } k_x + k_y = n_o \pi \\ \begin{pmatrix} 0 & 1 \\ 1 & 0 \end{pmatrix}, & k_x - k_y = n_o \pi \text{ or } k_x + k_y = n_e \pi. \end{cases} \quad (47)$$

Here  $n_{e(o)}$  is an even (odd) integer. Substituting these  $\hat{P}(k_y)$  into Eq. (40), we obtain  $\hat{L}$  as

$$\hat{L} \propto \frac{\text{sgn}(\Delta_A) + \text{sgn}(\Delta_B)}{|v_{Fx}|} \begin{pmatrix} 1 & 0 \\ 0 & 1 \end{pmatrix}. \quad (48)$$

The appearance condition of the ZBCP [Eq. (46)] is written as

$$\text{sgn}(\Delta_A) + \text{sgn}(\Delta_B) = 0, \quad (49)$$

on the lines where  $k_a=(k_x-k_y)/\sqrt{2}=n\pi$  or  $k_b=(k_x+k_y)/\sqrt{2}=n\pi$ . This condition is always satisfied in the sign-reversing  $s$ -wave ( $\pm s$ -wave) superconductors in this model. The  $\pm s$ -wave symmetry means that the symmetry of pair potentials on each Fermi surface is  $s$  wave and the relative phase between them is  $\pi$ .<sup>2-12</sup> Therefore, the ZBCP appears at the points on the Fermi surfaces where the relation  $k_a=0$  or  $k_b=0$  is satisfied in the momentum space.

### 2. Case of $t'/t=0$ for $[110]$ surface

In the case of  $t'/t=0$ , we can analytically show that the ZBCP always occurs for  $[110]$  surface. In this case, the unitary matrix  $\hat{P}$  can be written as

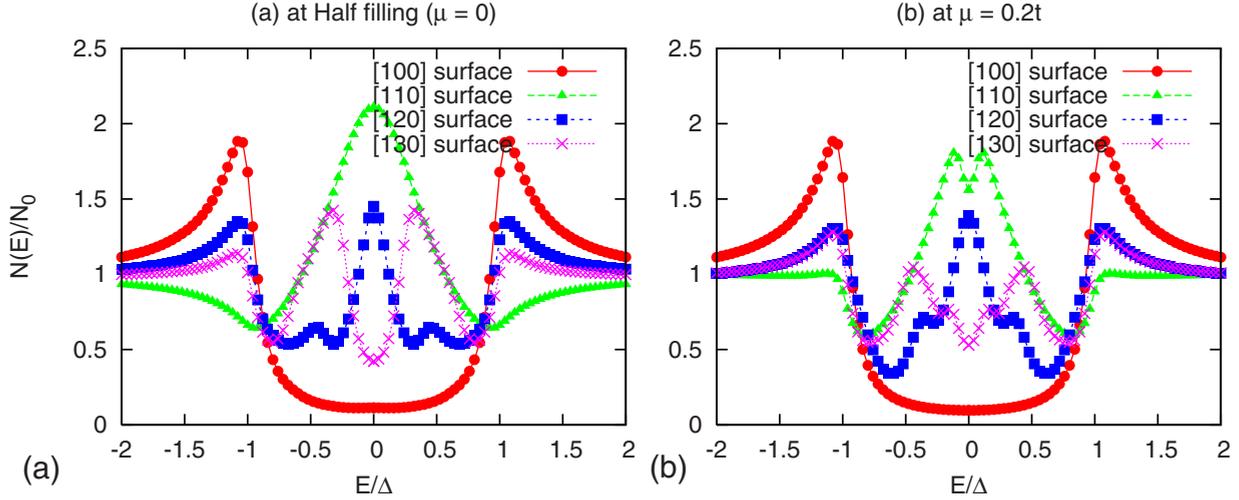


FIG. 5. (Color online) The density of states at the surface for various surface angles. The pair potentials are  $\Delta_A = \Delta = 0.001t$  and  $\Delta_B = -\Delta_A$ . (a) The half filling ( $\mu = 0$ ) and (b)  $\mu = 0.2t$ . The interorbital hopping amplitude is  $t' = 0.1t$ . The smearing factor is  $\eta = 0.1\Delta$ .

$$\hat{P}(k_y) = \begin{cases} \begin{pmatrix} 1 & 0 \\ 0 & 1 \end{pmatrix}, & k_x k_y > 0 \\ \begin{pmatrix} 0 & 1 \\ 1 & 0 \end{pmatrix}, & k_x k_y < 0. \end{cases} \quad (50)$$

As in the case of Eq. (47), these unitary matrices lead to the same appearance condition of the ZBCP as Eq. (49).

### 3. Case of $t'/t=0$ at the half filling for [110] surface

Finally, we discuss the difference between the appearance conditions with and without the quasiclassical approach. As shown in Appendix, the appearance condition obtained without the quasiclassical approach for  $t'=0$  at the half filling ( $k_y > 0$ ) is written as

$$\Delta_{ab} = 0, \quad (51)$$

$$I_1 = 0 \quad \text{or} \quad I_2 = 0, \quad (52)$$

where

$$I_{1,2} = \frac{\ln \left\{ \frac{[\sin(\pm k_y/\sqrt{2}) + \sqrt{1 + |\Delta_A/t|^2}]^2}{[\sin(\pm k_y/\sqrt{2}) - \sqrt{1 + |\Delta_A/t|^2}]^2} \right\}}{2\sqrt{1 + |\Delta_A/t|^2}},$$

$$- \frac{\ln \left\{ \frac{[\sin(\pm k_y/\sqrt{2}) + \sqrt{1 + |\Delta_B/t|^2}]^2}{[\sin(\pm k_y/\sqrt{2}) - \sqrt{1 + |\Delta_B/t|^2}]^2} \right\}}{2\sqrt{1 + |\Delta_B/t|^2}}, \quad (53)$$

$$\Delta_{ab} = -\pi \left( \frac{\text{sgn}(\Delta_B/t)}{\sqrt{1 + |\Delta_A/t|^2}} + \frac{\text{sgn}(\Delta_B/t)}{\sqrt{1 + |\Delta_B/t|^2}} \right). \quad (54)$$

Here we assume that the pair potentials  $\Delta_A$  and  $\Delta_B$  do not depend on  $k$  for simplicity. The above equations suggest that the appearance condition of the ZBCP depends on the details of the amplitudes  $|\Delta_A|$  and  $|\Delta_B|$  in contrast to the quasiclassical result [Eq. (49)]. In the limit of  $|\Delta_{A,B}/t| \ll 1$ , on the other hand, Eqs. (53) and (54) are reduced to Eq. (49) ob-

tained by the quasiclassical approximation. Thus the quasiclassical and nonquasiclassical results coincide in this limit. Therefore, it is suggested that our quasiclassical approach is appropriate when  $|\Delta_{A,B}|/t \ll 1$ .

## C. Numerical results

The density of states at the surface is calculated from Eq. (6) as

$$N(E) = \frac{1}{2\pi} \int dk_y N(x=0, k_y). \quad (55)$$

We consider the  $\pm s$ -wave superconductor<sup>2-12</sup> and the same two-band model as discussed in this section.

### 1. Dependence of the surface angle $\theta$

We show the energy dependence of the density of states for various surface angle  $\theta$  in Figs. 5 and 6. The peak positions of the Andreev bound states depend on the surface angle  $\theta$ . By comparing the results between Figs. 5 and 6, it is noticed that these positions do not depend on the pair-potential amplitude.

### 2. Dependence of the interband hopping amplitude $t'$

We investigate the dependence on the interorbital hopping amplitude  $t'$ . We consider [110] surface ( $\theta = \pi/4$ ). As shown in Fig. 7(a), the ZBCP always exists at the half filling ( $\mu = 0$ ) for any interband hopping amplitudes  $t'$ . At  $\mu = 0.2t$  as shown in Fig. 7(b), the ZBCP only appears when without an interband hopping, i.e.,  $t' = 0$ . These ZBCPs appear when the appearance condition in Eq. (49) is satisfied.

## V. DISCUSSION

The advantages of our method are that one can easily investigate the surface-angle dependence of the density of states with the use of the quasiclassical method and easily calculate the density of states in the  $n$ -band (multiband) sys-

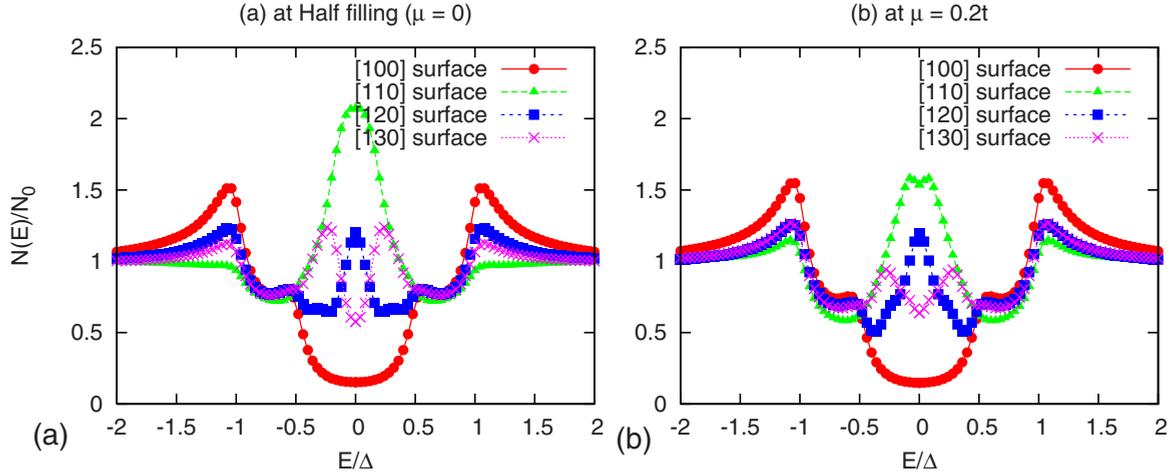


FIG. 6. (Color online) The density of states at the surface for various surface angles. The pair potentials are  $\Delta_A=\Delta=0.001t$  and  $\Delta_B=-0.5\Delta_A$ . (a) The half filling ( $\mu=0$ ) and (b)  $\mu=0.2t$ . The interorbital hopping amplitude is  $t'=0.1t$ . The smearing factor is  $\eta=0.1\Delta$ .

tem with less computational machine time. Therefore, we can take, for example, a realistic five-band model in order to discuss the density of states for iron-based superconductors. We will report its results in the near future.

We have assumed that the matrix of the pair potential in the band representation does not have off-diagonal elements which correspond to the interband pairings. When the interband pairing is dominant, the Cooper pairs have center-of-mass momentum  $q \neq 0$ . Usually such pairs are not energetically favorable since the pair potentials have spacial dependence even in bulk systems.

Starting with the same Matsumoto-Shiba method,<sup>26</sup> Onari *et al.*<sup>19</sup> recently calculated the surface Andreev bound states without the quasiclassical approximation. Their results show that the peak positions of the Andreev bound states depend on the gap amplitudes on two bands in the same two-band model as considered in this paper and the ZBCP does not always appear at the half filling. These results might seemingly be inconsistent with our quasiclassical results. It is, however, not the case.

Onari *et al.*<sup>19</sup> obtained the perturbed Green's function by directly integrating the original unperturbed Green's function over  $k_x$  and  $k_y$  numerically. The original unperturbed Green's function has sharp peaks on Fermi surfaces in the momentum space and rapid Fermi-wavelength oscillations in the real

space. We have integrated out those properties by the quasiclassical approximation. It should be noted that the pair potentials are of the order  $\Delta \sim 0.1t$  in Ref. 19. This parameter is out of our quasiclassical approach ( $\Delta/t \ll 1$ ). As shown in Sec. IV B 3, our analytical result, which depends on the details of the gap amplitudes and therefore is consistent with Ref. 19, is reduced to the quasiclassical result in the limit  $\Delta/t \ll 1$ . Thus, the differences in the obtained results between Onari *et al.*<sup>19</sup> and the present paper would be due to the difference in applicable parameter regions.

The formulation derived in Secs. II and III can be applied to general multiband superconductors including  $d$ -wave pairing superconductor. The appearance condition for the ZBCP is given as Eq. (39) in Sec. III. Let us consider, for instance, the case of the two-band model discussed in Sec. IV at the half filling for [110] surface. From Eq. (39), the appearance condition for the ZBCP is given as

$$\text{sgn}(\Delta_{A1}) + \text{sgn}(\Delta_{A2}) + \text{sgn}(\Delta_{B1}) + \text{sgn}(\Delta_{B2}) = 0. \quad (56)$$

Here  $\Delta_{A1}$  and  $\Delta_{A2}$  are the pair potentials on the inner Fermi surface (red) in Fig. 4, and  $\Delta_{B1}$  and  $\Delta_{B2}$  are the pair potentials on the outer Fermi surface (green) there. For a two-band  $d$ -wave superconductor,  $\Delta_{A1}=-\Delta_{A2}$  and  $\Delta_{B1}=-\Delta_{B2}$ , so that the above condition is satisfied and the ZBCP appears. Furthermore, in the case of a single-band  $d$ -wave supercon-

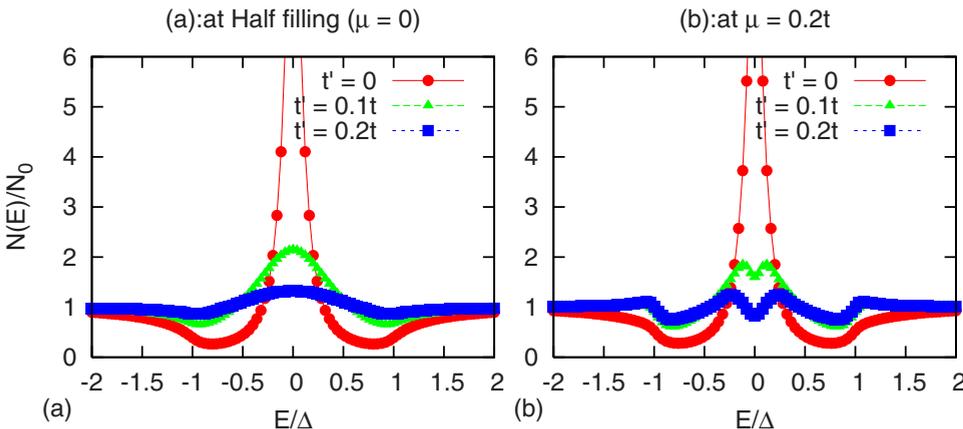


FIG. 7. (Color online) The density of states at [110] surface for various interorbital hopping amplitude  $t'$ . The pair potentials are  $\Delta_A=\Delta=0.001t$  and  $\Delta_B=-\Delta_A$ . (a) The half filling ( $\mu=0$ ) and (b)  $\mu=0.2t$ . The smearing factor is  $\eta=0.1\Delta$ .

ductor, the appearance condition for the ZBCP is obtained from Eq. (39) as

$$\text{sgn}(\Delta_{A1}) + \text{sgn}(\Delta_{A2}) = 0. \quad (57)$$

This is consistent with previous results for  $d$ -wave pairing in Refs. 13–15 and 26 where the ZBCP appears when the quasiparticles feel a superconducting phase change  $\pi$  in the surface-scattering process  $A1 \leftrightarrow A2$  on a Fermi surface.

## VI. CONCLUSION

In conclusion, we extended the single-band method by Matsumoto and Shiba<sup>26</sup> into general  $n$ -band case ( $n \geq 2$ ). With the use of the quasiclassical approximation, we developed the way to integrate the unperturbed Green's function with respect to  $k_x$  which is the momentum component perpendicular to a surface. We showed that the appearance condition of the ZBCP does not depend on any anisotropy in the pair-potential amplitude, but only on the relative phase, in the case of  $\Delta \ll E_F$  in  $n$ -band systems. The properties of the normal state are influential for the ZBCP to appear.

We also calculated the surface density of states in the two-band system as a simple example of our approach. We suggested that our quasiclassical approach is appropriate when  $|\Delta|/t \ll 1$ . We showed that the peaks of the density of states due to the Andreev bound states depend on the surface angle and the parameters in the normal state ( $t, t', \mu$ ) so that the sign-reversing  $s$ -wave ( $\pm s$ -wave) superconductors exhibit complicated properties in the tunneling spectroscopy compared to single-band  $d$ -wave superconductors.

## ACKNOWLEDGMENTS

We thank Y. Kato, M. Machida, N. Nakai, H. Nakamura, M. Okumura, C. Iniotakis, M. Sigrist, Y. Tanaka, and S. Onari for helpful discussions and comments. Y.N. acknowledges support by Grant-in-Aid for JSPS (Grant No. 204840). N.H. was supported by JSPS Core-to-Core Program-Strategic Research Networks, nanoscience and engineering in superconductivity (NES).

## APPENDIX: INTEGRATION WITHOUT QUASICLASSICAL APPROXIMATION

We will show the ZBCP appearance condition Eqs. (51) and (52) for zero interorbital hopping amplitude ( $t'=0$ ) by integrating Eq. (25) in the simple two-band model for [110] surface at the half filling.<sup>27</sup>

The Hamiltonian in the normal state is described as

$$\hat{H}^o = \begin{pmatrix} \epsilon_1(\tilde{k}_x, \tilde{k}_y) & 0 \\ 0 & \epsilon_2(\tilde{k}_x, \tilde{k}_y) \end{pmatrix}, \quad (A1)$$

with

$$\epsilon_1(\tilde{k}_x, \tilde{k}_y) = -t \cos(\tilde{k}_x - \tilde{k}_y), \quad (A2)$$

$$\epsilon_2(\tilde{k}_x, \tilde{k}_y) = -t \cos(\tilde{k}_x + \tilde{k}_y). \quad (A3)$$

Here we have introduced  $\tilde{k}_x = k_x/\sqrt{2}$  and  $\tilde{k}_y = k_y/\sqrt{2}$ . Considering the pair potentials  $\Delta_{A,B}$  which do not depend on  $\mathbf{k}$  and

using the unitary matrix [Eq. (50)], the pair-potential matrix in the orbital representation can be written as

$$\hat{\Delta}^o = \begin{pmatrix} \Delta_A \theta(\tilde{k}_x) + \Delta_B \theta(-\tilde{k}_x) & 0 \\ 0 & \Delta_A \theta(\tilde{k}_x) + \Delta_B \theta(-\tilde{k}_x) \end{pmatrix} \\ \equiv \begin{pmatrix} \Delta_{\tilde{k}_x} & 0 \\ 0 & \Delta_{-\tilde{k}_x} \end{pmatrix}. \quad (A4)$$

The unperturbed retarded Green's function  $\check{G}_0^R(E, k_x, k_y)$  is written as

$$\check{G}_0^R(E, \tilde{k}_x, \tilde{k}_y) = (E - \check{H}_N^o)^{-1} = \begin{pmatrix} \hat{A}_+ & \hat{B} \\ \hat{B} & \hat{A}_- \end{pmatrix}, \quad (A5)$$

where

$$\hat{A}_\pm = \begin{pmatrix} \frac{E \pm \epsilon_1}{-|\Delta_{\tilde{k}_x}|^2 + E^2 - \epsilon_1^2} & 0 \\ 0 & \frac{E \pm \epsilon_2}{-|\Delta_{\tilde{k}_x}|^2 + E^2 - \epsilon_2^2} \end{pmatrix}, \quad (A6)$$

$$\hat{B} = \begin{pmatrix} \frac{\Delta_{\tilde{k}_x}}{-|\Delta_{\tilde{k}_x}|^2 + E^2 - \epsilon_1^2} & 0 \\ 0 & \frac{\Delta_{-\tilde{k}_x}}{-|\Delta_{\tilde{k}_x}|^2 + E^2 - \epsilon_2^2} \end{pmatrix}. \quad (A7)$$

To investigate the appearance condition of the ZBCP, we set  $E=0$  (i.e., zero energy),  $x=0$  and  $x'=0$  (i.e., at the surface). Then, we calculate  $\check{G}_0^R(E=0, x=0, x'=0, k_y)$  as

$$\check{G}_0^R(E=0, x=x'=0, \tilde{k}_y) = \int_{-\pi}^{\pi} \frac{d\tilde{k}_x}{2\sqrt{2}\pi} \check{G}_0^R(E=0, \tilde{k}_x, \tilde{k}_y). \quad (A8)$$

Each element in this matrix can be integrated analytically as

$$\int \frac{d\tilde{k}_x \cos(\tilde{k}_x \pm \tilde{k}_y)}{|\Delta|^2 + \cos^2(\tilde{k}_x \pm \tilde{k}_y)} = \int \frac{-dx}{|\Delta|^2 + 1 - x^2}, \quad (A9)$$

$$\int \frac{d\tilde{k}_x}{|\Delta|^2 + \cos^2(\tilde{k}_x \pm \tilde{k}_y)} = \int \frac{dx \frac{1}{1+x^2}}{|\Delta|^2 + \frac{1}{1+x^2}}. \quad (A10)$$

Integrating  $\check{G}_0^R(E=0, \tilde{k}_x, \tilde{k}_y)$  by using the above formulae, we finally obtain  $\check{G}_0^R(E=0, x=0, x'=0, k_y)$  as



$$\check{G}_0^R(E=0, x=0, x'=0, k_y) \propto \frac{1}{t} \begin{pmatrix} -I_1 & 0 & \Delta_{ab} & 0 \\ 0 & -I_2 & 0 & \Delta_{ab} \\ \Delta_{ab} & 0 & I_1 & 0 \\ 0 & \Delta_{ab} & 0 & I_2 \end{pmatrix}, \quad (\text{A11})$$

where  $I_{1,2}$  and  $\Delta_{ab}$  are defined in Eqs. (53) and (54). Its inverse matrix is written as

$$[\check{G}_0^R]^{-1} \propto t \begin{pmatrix} \frac{-I_1}{(\Delta_{ab})^2 + I_1^2} & 0 & \frac{\Delta_{ab}}{(\Delta_{ab})^2 + I_1^2} & 0 \\ 0 & \frac{-I_2}{(\Delta_{ab})^2 + I_2^2} & 0 & \frac{\Delta_{ab}}{(\Delta_{ab})^2 + I_2^2} \\ \frac{\Delta_{ab}}{(\Delta_{ab})^2 + I_2^2} & 0 & \frac{I_1}{(\Delta_{ab})^2 + I_1^2} & 0 \\ 0 & \frac{\Delta_{ab}}{(\Delta_{ab})^2 + I_2^2} & 0 & \frac{I_2}{(\Delta_{ab})^2 + I_1^2} \end{pmatrix}. \quad (\text{A12})$$

The zero-energy bound states appear when  $[\check{G}_0^R]^{-1}$  diverges as noticed from Eqs. (4) and (5). Therefore, the appearance condition of the ZBCP is expressed as

$$\Delta_{ab} = 0, \quad (\text{A13})$$

$$I_1 = 0 \text{ or } I_2 = 0. \quad (\text{A14})$$

- 
- <sup>1</sup>Y. Kamihara, T. Watanabe, M. Hirano, and H. Hosono, *J. Am. Chem. Soc.* **130**, 3296 (2008).  
<sup>2</sup>I. I. Mazin, D. J. Singh, M. D. Johannes, and M. H. Du, *Phys. Rev. Lett.* **101**, 057003 (2008).  
<sup>3</sup>K. Kuroki, S. Onari, R. Arita, H. Usui, Y. Tanaka, H. Kontani, and H. Aoki, *Phys. Rev. Lett.* **101**, 087004 (2008).  
<sup>4</sup>M. M. Korshunov and I. Eremin, *Phys. Rev. B* **78**, 140509(R) (2008).  
<sup>5</sup>K. Seo, B. A. Bernevig, and J. Hu, *Phys. Rev. Lett.* **101**, 206404 (2008).  
<sup>6</sup>T. Nomura, *J. Phys. Soc. Jpn.* **77**, Suppl. C, 123 (2008), <http://jpsj.ipap.jp/link?JPSJS/77SC/123/>; *J. Phys. Soc. Jpn.* **78**, 034716 (2009).  
<sup>7</sup>Y. Bang and H.-Y. Choi, *Phys. Rev. B* **78**, 134523 (2008).  
<sup>8</sup>M. M. Parish, J. Hu, and B. A. Bernevig, *Phys. Rev. B* **78**, 144514 (2008).  
<sup>9</sup>R. Arita, S. Onari, H. Usui, K. Kuroki, Y. Tanaka, H. Kontani, and H. Aoki, *J. Phys.: Conf. Ser.* **150**, 052010 (2009).  
<sup>10</sup>V. Stanev, J. Kang, and Z. Tesanovic, *Phys. Rev. B* **78**, 184509 (2008).  
<sup>11</sup>Y. Senga and H. Kontani, *J. Phys. Soc. Jpn.* **77**, 113710 (2008).  
<sup>12</sup>Y. Nagai, N. Hayashi, N. Nakai, H. Nakamura, M. Okumura, and M. Machida, *New J. Phys.* **10**, 103026 (2008).  
<sup>13</sup>C. R. Hu, *Phys. Rev. Lett.* **72**, 1526 (1994).  
<sup>14</sup>Y. Tanaka and S. Kashiwaya, *Phys. Rev. Lett.* **74**, 3451 (1995).  
<sup>15</sup>S. Kashiwaya and Y. Tanaka, *Rep. Prog. Phys.* **63**, 1641 (2000).  
<sup>16</sup>H.-Y. Choi and Y. Bang, arXiv:0807.4604 (unpublished).  
<sup>17</sup>A. A. Golubov, A. Brinkman, O. V. Dolgov, I. I. Mazin, and Y. Tanaka, arXiv:0812.5057 (unpublished).  
<sup>18</sup>M. A. N. Araújo and P. D. Sacramento, *Phys. Rev. B* **79**, 174529 (2009).  
<sup>19</sup>S. Onari and Y. Tanaka, *Phys. Rev. B* **79**, 174526 (2009).  
<sup>20</sup>D. Wang, Y. Wan, and Q.-H. Wang, arXiv:0901.1419 (unpublished).  
<sup>21</sup>J. Linder, I. B. Sperstad, and A. Sudbø, arXiv:0901.1895 (unpublished).  
<sup>22</sup>J. Linder and A. Sudbø, *Phys. Rev. B* **79**, 020501(R) (2009).  
<sup>23</sup>W.-F. Tsai, D.-X. Yao, B. A. Bernevig, and J. P. Hu, arXiv:0812.0661 (unpublished).  
<sup>24</sup>P. Ghaemi, F. Wang, and A. Vishwanath, *Phys. Rev. Lett.* **102**, 157002 (2009).  
<sup>25</sup>K. A. Yates, K. Morrison, J. A. Rodgers, G. B. S. Penny, J.-W. G. Bos, J. P. Attfield, and L. F. Cohen, *New J. Phys.* **11**, 025015 (2009), see Table I and references therein.  
<sup>26</sup>M. Matsumoto and H. Shiba, *J. Phys. Soc. Jpn.* **64**, 1703 (1995).  
<sup>27</sup>We have confirmed that one can analytically integrate Eq. (25) in this model for [110] surface also at *non-half-filling* ( $\mu \neq 0$ ).